

Performance and Analysis of Different Photovoltaic Technologies at Selected Sites

**Prepared for the
U.S. Department of Energy
Office of Electricity Delivery and Energy Reliability**

**Under Cooperative Agreement No. DE-EE0003507
Hawai‘i Energy Sustainability Program**

**Subtask 3.1 Photovoltaic Systems: Report 1 -- Field Testing and
Evaluation of Photovoltaic Technologies**

**Submitted by
Hawai‘i Natural Energy Institute
School of Ocean and Earth Science and Technology
University of Hawai‘i**

September 2014

Acknowledgement: This material is based upon work supported by the United States Department of Energy under Cooperative Agreement Number DE-EE0003507.

Disclaimer: This report was prepared as an account of work sponsored by an agency of the United States Government. Neither the United States Government nor any agency thereof, nor any of their employees, makes any warranty, express or implied, or assumes any legal liability or responsibility for the accuracy, completeness, or usefulness of any information, apparatus, product, or process disclosed, or represents that its use would not infringe privately owned rights. Reference here in to any specific commercial product, process, or service by trade name, trademark, manufacturer, or otherwise does not necessarily constitute or imply its endorsement, recommendation, or favoring by the United States Government or any agency thereof. The views and opinions of authors expressed herein do not necessarily state or reflect those of the United States Government or any agency thereof.

Performance and analysis of different PV technologies at selected sites

Contents

1	Introduction	2
2	Data management and analysis tools.....	2
2.1	Data server	2
2.2	Database	3
2.3	Data visualization and analysis	4
3	PV System Performance	6
3.1	Puu Waa Waa (PWW), Hawaii	6
3.1.1	Solar resource	7
3.1.2	Performance of the PV systems.....	9
3.2	Green Holmes Hall Initiative (GHHI), Oahu.....	16
3.2.1	Solar resource	17
3.2.2	Performance of the PV systems.....	19
4	Conclusions	23
5	References	25

1 Introduction

Under previous funding from the US Department of Energy (DOE)(Award No DE-FC26-06NT42847), the Hawaii Natural Energy Institute (HNEI) at the University of Hawaii at Manoa (UH) deployed photovoltaic (PV) test beds to evaluate the performance of a variety of PV systems operating under varying environmental conditions in various locations in Hawaii. Site selection and the test protocols were described in detail in the Final Technical Report under that award: “PV Test Sites and Test Protocols” [1]. Performance of the PV systems during the first year of operation was presented in the Final Technical Report titled: “Solar resource and PV Systems Performance at Selected Test Sites” [2]. The grid-connected sites used for this testing included Puu Waa Waa ranch on the Island of Hawaii (PWW), on the roof of Holmes Hall at the UH Manoa campus (GHHI) and at the UH Maui campus (UHMC).

Under this award (#DE-EE0003507), HNEI has improved the data acquisition and databasing, and continued to collect and analyze data at two of the three sites. HNEI has developed and implemented a methodology to streamline data acquisition and databasing. Specifically, the collection of the performance data from the data acquisition systems (DAS) at the different test locations has been automated to feed a NetCDF-formatted database. This multi-domain data format improves database access by the MATLAB data visualization and analysis tools. During the past year, HNEI collected a second year of operation and performance data at Puu Waa Waa (PWW) and Holmes Hall (GHHI). Both efforts are summarized in this report.

2 Data management and analysis tools

The data collected at the PV test sites are transferred to a data server where they are stored and analyzed. The network architecture required between all DAS and the data server was carefully selected allowing secure, automated data file transfer. Once in the data server, the data files are converted into a database for easy access of the datasets by the data visualization and analysis tools. These efforts are described in more detail below.

2.1 Data server

A data server was deployed at UH Manoa campus. It has a CentOS 5.5 operating system and consists of the following equipment:

- Dual Xeon E5620 2.4-GHz Quad Core
- 6-GB DDR3 1333MHz RAM
- 16 x 2 TB drives in RAID 6 configuration.

The data server was enhanced by the addition of:

- 48 GB RAM to increase the calculation capability and
- A Network Attached System (NAS) with 30 TB drives to back up the data files and provide an easy to use remote file access system without exposing the original data.

A Virtual Private Network (VPN) firewall architecture has been implemented at each PV test bed and at the server to provide a secured network. The data server and NAS are behind a dual layer of firewalls. The UH School of Ocean and Earth Science and Technology (SOEST) firewalls provide intrusion prevention and a first layer of protection, while the HNEI firewall provides protection if someone on the SOEST network exposes the network to malware, and provides VPN access over VPN tunnels to other firewalls. These are both enterprise grade firewalls that meet or exceed the requirements of the Federal Information Security Management Act.

The data files from the DAS are downloaded daily via File Transfer Protocol (FTP). The data download is automated using a Cron job, a Linux command for scheduling a command or script on a server to complete repetitive tasks automatically. The data server is running custom scripts that connect to the PV sites to harvest data and are run in a staggered fashion to avoid overwhelming the host institutions' networks.

2.2 Database

The data files are transferred daily from the different test sites as text files. In most instances the data is collected at a 1-second time step. A custom designed HNEI DAS collects up to 80 data points on Hawaii, 30 on Maui, and 60 on Oahu corresponding to the DC current and voltage for each PV module and string of PV array, as well as environmental measurements. For more information on the data which is collected, refer to the instrumentation of the PV test beds described in the previous report [1].

The data files are converted into a NetCDF data format, a multi-domain scientific data format, using MATLAB. NetCDF [3], widely used by the scientific community, is a set of software libraries and self-describing, machine-independent data formats that support the creation, access, and sharing of array-oriented scientific data. MATLAB provides access functions to NetCDF data files.

The original datasets collected by the DAS are converted into performance datasets used for the analysis using a two-step process. First, the NetCDF datasets corresponding to the raw data are visualized to evaluate the proper operation of the sensors and to select the data to be used for the calculation of the performance of the PV systems. The second NetCDF datasets correspond to the selected performance data of the PV systems, including information on the solar resource and environment that are needed for the analysis. The selected performance data is identical for all PV systems allowing using the same analysis tool for all PV systems and locations. Table 1 describes the selected datasets used for the analysis presented in this report. It includes the DC current, voltage and power, monitored or calculated, and the solar radiation or irradiance monitored by the thermopile pyranometer or averaged from the signals of the solar cell pyranometers surrounding the PV test beds. Additional measurements or calculations can be added to the selected datasets when needed for the analysis.

Table 1: Selected datasets used for the analysis

Selected Dataset	Description
Date & Time	Provided by the DAS time-synchronized controller
DC Current	Monitored or calculated by adding string currents
DC Voltage	Monitored or calculated by averaging string voltages
DC Power	Calculated from DC current and DC voltage
Irradiance	Monitored by the thermopile pyranometer
Irradiance	Monitored by the Solar Cell pyranometers and averaged using the multiple sensors surrounding the PV installations

2.3 Data visualization and analysis

Visualization of the performance datasets is essential to understand the operation of the PV systems and to define periods of operation that can be used for the performance analysis. It was important to recognize periods of shading of the PV systems occurring at all test sites, either affecting all PV systems at the site due to seasonal shading (observed at PWW, due to the natural topography of the site), or with different impact on the PV systems operating at the same location due to local shading (observed at GHHI, due to a nearby building shading one of the arrays). The impact of the shading was removed at all sites to evaluate and compare the performance of the PV systems in normal operation. Shading due to the clouds is included in the analysis. Removing seasonal shading is done by limiting the analysis to spring and summer months, as will be explained later. Local shading is eliminated by reducing the hours of operation between 9AM and 4PM.

Data analysis determines on a daily basis the PV system performance by averaging and integrating (energy) the performance data. We evaluate the daily performance, the performance per levels of irradiance and the 5-minute average performance used for visualization. The analysis considers the datasets with solar radiation above 125 W/m² to maximize the signal to noise ratio of the pyranometer. The performance of the PV systems is estimated using the performance ratio (PR), defined as the ratio of the PV yield by the solar yield (Equation 1). The PV yield is the PV energy production per watt peak, power rating of the PV system defined by the specifications at standard test conditions (STC). The solar yield or sun peak hour is the solar energy in Wh per square meter divided by the STC irradiance.

$$PR = \frac{Y_{PV}}{Y_{Sun}} = \frac{\frac{E_{PV}}{P_{PV,STC}}}{\frac{E_{Sun}}{SR_{STC}}} \quad \text{Equation 1}$$

With	PR	Performance ratio [%]
	Y_{PV}	PV yield [Wh/W or h]
	Y_{Sun}	Solar yield or sun peak hours [h]
	E_{PV}	PV energy [Wh]
	$P_{PV,STC}$	PV power rating specified by the manufacturer at STC [W]
	E_{Sun}	Solar energy [Wh/m ²]
	SR_{STC}	Irradiance at the STC [= 1,000 W/m ²]

The PR defines how well a PV system performs in comparison to its theoretical production at STC. The following analysis evaluates the DC PR, which does not take into account the loss in the inverter. The analysis results present the solar energy and the PR of the PV systems calculated for different periods of analysis (yearly, monthly,...) or for selected days such as cloudy or sunny days. Presentation of the results per levels of irradiance is helpful to understand the performance differences between PV systems.

Solar irradiance used for the analysis under the previous award was measured using silicon solar cell pyranometers because of their fast response. For this study, we used the thermopile pyranometer because of its accurate reading of the total available solar radiation. Analysis results are sensitive to the type of solar sensor due to different spectral response and to the cosine error of the solar cell pyranometer varying as a function of zenith angle and temperature [5]. Figure 1 shows the yearly PR profile of the polycrystalline PV array operating at the test site in Oahu comparing the results obtained using different types of pyranometers for the analysis. To compare with last reported results, we used the dataset from October 2011 to September 2012. The PR versus irradiance plot calculated with the solar cell sensor (SR) is similar to that previously reported (Figure 15 in [2]). At high irradiance levels above 600 W/m² (low zenith angle), the PR is estimated lower when using the thermopile sensor suggesting that the solar cell sensor underestimates the irradiance, likely due to the temperature. At low levels of irradiance below 500 W/m², the solar cell pyranometer overestimates the irradiance due to the cosine error important at high zenith angles. Thus, the PR at low irradiance levels was underestimated during the last analysis. Corrections are provided in this report.

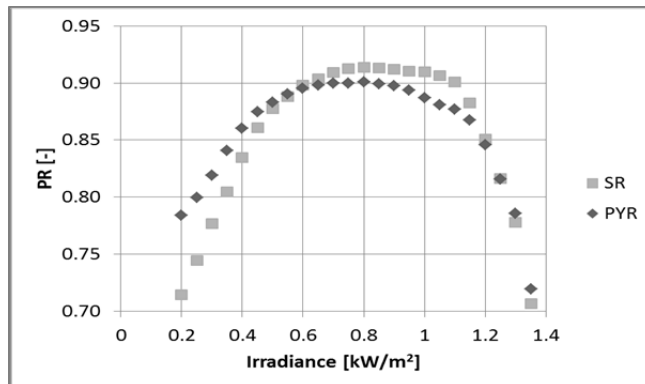


Figure 1: Yearly PR as a function of levels of irradiance using the solar cell pyranometers (SR) or the thermopile pyranometer (PYR) – Polycrystalline PV array operating at GHHI from October 2011 to September 2012.

During this phase of the work, the analysis was limited to the sites on Oahu (GHHI) and on Hawaii (PWW), as these two sites offer side-by-side comparison of PV systems with identical PV system configurations but with different PV module technologies. We do not include the test site on Maui that consists of three PV arrays of polycrystalline modules from the same PV and inverter manufacturers. The Maui site experiences important noise levels, estimated at 50-85 W/m², on the thermopile pyranometer, preventing the correction on the PR plots per levels of irradiance.

3 PV System Performance

In the next sections, we present a summary of the PV test site installations followed by the description of the solar resource and the analysis of the PV system performance and parameters.

3.1 Puu Waa Waa (PWW), Hawaii

The test site at PWW [5, 6] is a sparsely populated location on the North end of the Kona Coast on the Island of Hawaii (Latitude: 19.8°N, Longitude: 155.8°W, Altitude: 686 m). The test bed lies on the western slope of the largest volcanoes, Mauna Kea and Mauna Loa, and on the northern flank of Hualalai Mountain, at the bottom of the cinder cone called Puu Waa Waa (Figure 2).



Figure 2: PWW, Kona Coast of Hawaii – PV systems ground mounted on open rack structures (left) at the bottom of the Puu Waa Waa cinder cone (right)

Table 2 describes the PV modules selected for testing at PWW. The PV technologies are three-junction amorphous from Uni-Solar (UN), polycrystalline from BP Solar (BP), monocrystalline from SolarWorld (SW), and from Suntech (ST), and heterojunction with intrinsic layer (HIT) module from SANYO (SA). SANYO HIT modules have been supplied by PANASONIC since April 2012. Two PV modules from each manufacturer were purchased and tested individually using micro inverters.

Table 2: Description of the PV modules tested PWW in the Island of Hawai'i

PV Module Manufacturers	PV Module Model Number	PV Technology	STC Module Efficiency [%]	STC Peak Power [W]
SANYO (SA)	HIP-210NKA5	HIT (Amorphous and Monocrystalline)	16.7	210
BP Solar (BP)	BP175B	Polycrystalline	13.9	175
Suntech Power (ST)	STP 175S-24/Ab-1	Monocrystalline	13.7	175
SolarWorld (SW)	SW175-P	Monocrystalline	13.4	175
Uni-Solar (UN)	PVL-68	Amorphous (flexible)	6.1	68

Table 3 provides additional information on the PV systems tested at PWW including information on the inverter, the PV system configuration, and the type of mounting system. Two models of micro inverters from Enphase (M190 and M210) are used to connect the PV modules. The flexible modules from Uni-Solar require connecting two modules in series to match the MPPT voltage range and recommended power of the micro inverter. The PV modules are ground mounted, with a 20° tilt, facing south, on open

rack structures. The flexible modules are installed on a small standing seam roof, with a 20° tilt, facing south.

Table 3: Tested PV systems at PWW in the Island of Hawai‘i : Inverter, PV system configuration and PV module mount.

PV	Inverter			PV system configuration			PV Module Mounting
	Type	Brand	Power [W]	# of inverters	# of PV modules	PV arrangement per inverter	
BP	Micro	Enphase	190	2	2	PV individually tested	Open rack
SA	Micro	Enphase	210	2	2	PV individually tested	Open rack
SW	Micro	Enphase	190	2	2	PV individually tested	Open rack
ST	Micro	Enphase	190	2	2	PV individually tested	Open rack
UN	Micro	Enphase	190	2	4	2 PV in series	Roof

The PWW PV test bed and associated data acquisition system (DAS) were commissioned in July of 2010. The test bed operated for almost three years until March 2013, but suffered from many interruptions in terms of PV operation and data transmission from March 2012. The following results correspond to a 21-month period of analysis from July 2010 to March 2012. It includes 595 days of analysis. Data loss (~5%) is related to missing datasets due to failure of the DAS, or loss of communication. The datasets were also limited to properly operating PV systems (removing periods of grid shortage, or inverter failure) and to periods of operation common to all PV systems at the test site.

3.1.1 Solar resource

Figure 3 shows the variation of the daily average irradiation recorded at the PWW test site by the thermopile pyranometer during the 21-month period of analysis from July 2010 to March 2012. The graph also includes the monthly values of the average and standard deviation of the irradiation. The daily irradiation is similar during the two years of analysis, varying wildly over the year and averaging 3.6 kWh/m²/day. The monthly variation of the irradiation has peaks at the equinox in September and March and lower values during the solstice months. The standard deviation is similar along the period of analysis, averaging 1.2 kWh/m²/day. The monthly variation and the small seasonal variation are related to the latitude of the site and the tilt of the measurements in the plane of the PV modules (20° tilt).

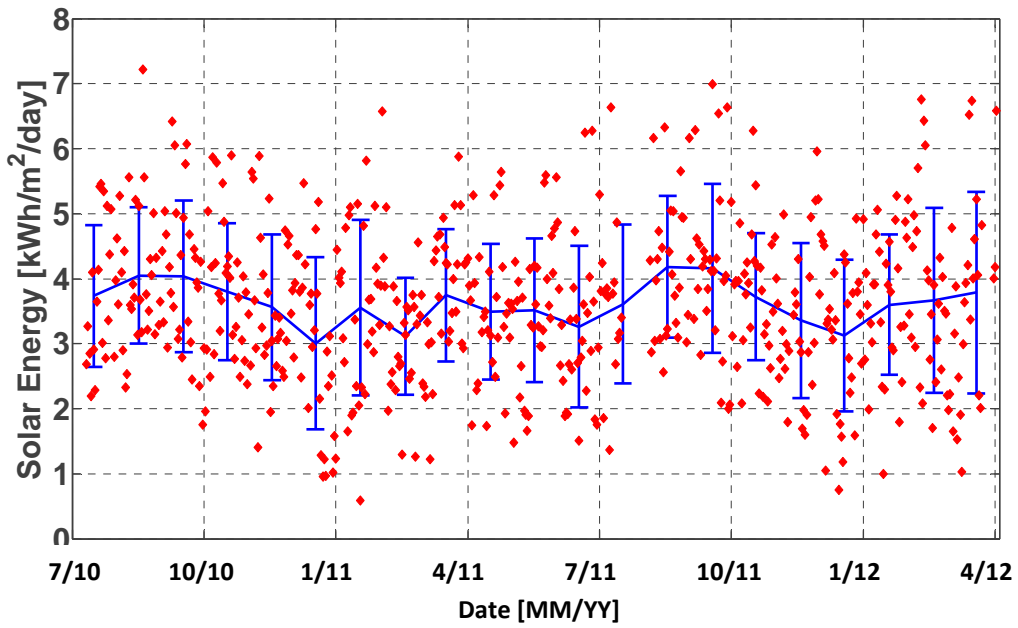


Figure 3: Daily average irradiation at PWW, Hawaii for 21 months of recording from July 2010 till March 2012. Also shown are monthly averages and standard deviation bars.

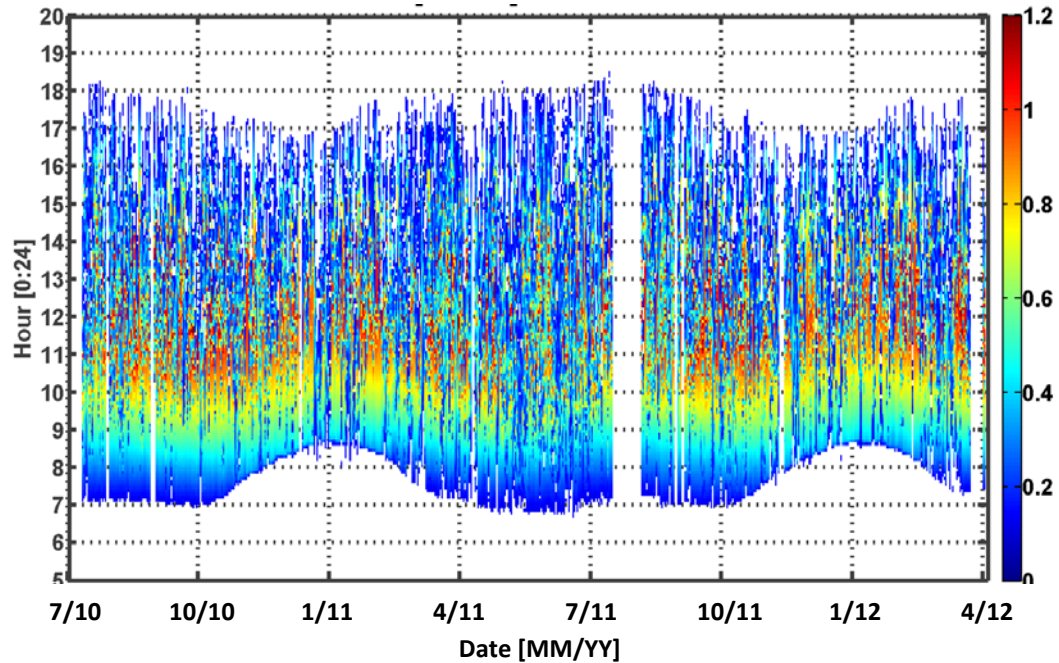


Figure 4 Solar maps at PWW, Hawaii: five-minute average solar radiation [kW/m^2] varying as a function of hours of the day (y-axis) during the 21-month period of analysis (x-axis) from July 2010 till March 2012

Five-minute average solar radiation as a function of hour of the day (y-axis) during the period of analysis (x-axis) is shown in Figure 4. The colors give the level of the solar radiation or irradiance in kW/m^2 in accordance with the color bar on the right. There is no data available before 7 AM and after 6 PM

because the analysis does not take into account the datasets collected with irradiance levels below 125 W/m², to maximize the signal of the pyranometer to noise ratio. The dawn and dusk lines vary with the day of the year, which is related to the earth-sun tilt and local shading. PWW experiences important shading during the months of fall and winter, affecting the irradiance in the morning up until 8:45 AM in December, due to the Puu Waa Waa cinder cone located South East of the PV test bed (Figure 2).

The 21-month average and standard deviation of the solar radiation estimated as a function of the time of day are plotted in Figure 5. The solar radiation increases regularly from 7 AM reaching 600 W/m² at 10 AM with a relatively small deviation indicating consistency of mostly clear sky in the mornings. After 10 AM, the cloud cover becomes predominant. The average irradiance stays constant until 11 AM and decreases in the afternoon. This site is found to be dominated by afternoon clouds that significantly attenuate solar irradiance.

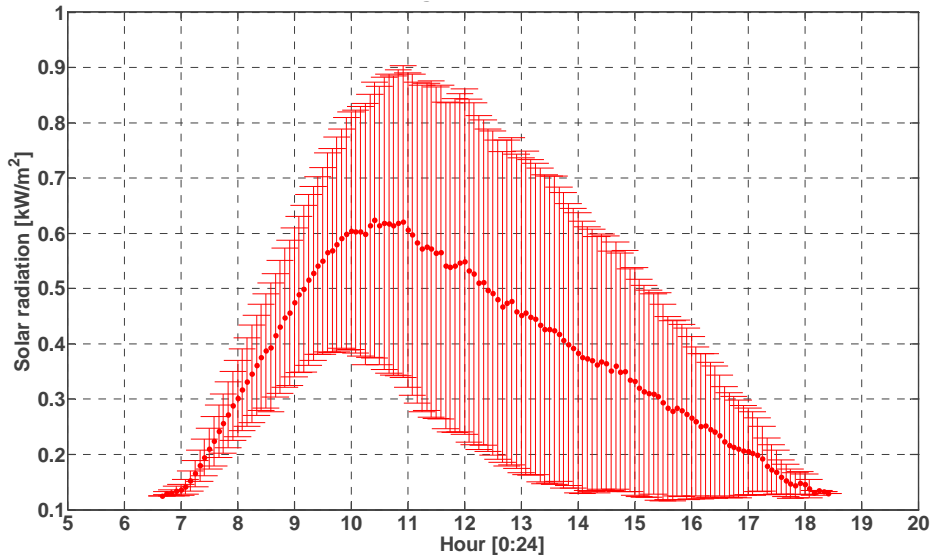


Figure 5: 21-month average and standard deviation of the solar radiation at PWW as a function of the time of the day.

3.1.2 Performance of the PV systems

The morning shading during fall and winter months has an impact on the performance of the PV modules operating at PWW, especially on the PR versus irradiance plots used to understand the performance differences between PV systems. In order to eliminate the impact of the seasonal shading at the site, we limited the analysis to the spring and summer months (from July to September 2010 and from March to September 2011). We used these datasets for the analysis of the average performance and the impact of the weather conditions presented in the next two sections. We complete the analysis by evaluating the variation of the performance and impact of the weather conditions during the full 21-month period of operation.

3.1.2.1 Average performance

Table 4 describes the average PR of the PV modules tested at PWW during the period of analysis - i.e., spring/summer months between July 2010 and March 2012. The second column gives the standard deviation of the average PR between the two sample modules tested in identical conditions (same PV module specification, same micro inverter).

Table 4: Average PR of the PV modules tested at PWW during the spring and summer months from July 2010 till March 2012 - Standard deviation of the average PR between the 2 tested PV modules (STD(PV)).

PV	Average	STD(PV)
SW	96.8%	0.1%
SA	93.8%	1.8%
ST	91.3%	0.6%
UN	91.2%	0.4%
BP	89.2%	0.6%

At PWW, the SW monocrystalline module has the highest PR with 96.8%. The BP polycrystalline modules have the lowest performance at the site estimated at 89.2%. The standard deviation of the average PR between the two PV modules from the same manufacturer is estimated to be less than 0.6% for most of the PV modules tested at PWW. Only the HIT modules from SA have a high standard deviation between the two tested modules, estimated at 1.8%. The deviation of the performance of PV modules from the same manufacturer is not an issue at the PWW site as the PV modules are tested individually with micro inverters. It can lead to a more important loss called mismatch loss in array configuration. The difference between actual module power and the power rating specified in the datasheet is also important in terms of impacting the average PR values. To investigate the performance deviation, we requested the flash test results (FTR) that are available from the manufacturers via the serial number of the PV modules. SW responded to our request. The FTR performances are very similar between the two tested SW modules, which lead to small performance differences when the two SW modules operate at PWW (standard deviation $\sim 0.1\%$). The FTR power rating (178 W) is estimated higher (by 1.7%) than the datasheet power rating (175 W). Adjusting for the actual power rating of the SW modules decreases the estimated PR by 1.7% (Equation 1), leading to an actual corrected PR of 95.1%. Unfortunately, the other manufacturers did not reply to our request for FTR. The PR values presented in this report are therefore limited to the performance of the PV modules compared to the STC power rating provided in the datasheet. In future experiments, the PR should also be evaluated using the actual power of the PV modules using the FTR power rating or by using an IV tracer on site.

The average PR at all irradiance levels for the PV modules tested at PWW during spring/summer months of the test period is shown in Figure 6. These results are different than previously reported due to the impact of the shading and the use of the solar cell pyranometer in the previous analysis. For all PV modules, the PR decreases with increasing irradiance levels from 700 W/m^2 until saturation of the inverter dropping the PR above 1.1 kW/m^2 for the SA and 1.3 kW/m^2 for the crystalline modules. No

inverter saturation was observed for the UN. The saturation of the inverters varies between modules due to different sizing of the PV systems (PV power compared to inverter DC power). The impact of the saturation of the inverters was estimated to be negligible (< 0.1% variation of the average PR) during the last analysis. The slope of the PR versus irradiance plots at high irradiance varies with the PV technology. This is related to the peak power temperature coefficient (TC) of the PV modules (usually available in datasheet), lower for the amorphous (TC: 0.2%/°C) and HIT (TC: 0.3%/°C) modules compared to the crystalline (TC: 0.5%/°C). Below 700 W/m², the variation of the PR with the irradiance levels depends on the PV technology. For the monocrystalline modules, the PR decreases with increasing irradiance levels. For the HIT module, the PR is about constant from 250 W/m² to 700 W/m² with degradation of the performance at 200 W/m². The PR of the BP and UN modules increases with increasing irradiance levels reaching a peak PR at 550 W/m² for the polycrystalline and 700 W/m² for the amorphous. The PR versus irradiance plots of the two monocrystalline modules have similar shapes. The performance of the SW is higher than the ST at all levels of irradiance with a PR difference estimated at 6% at 200 W/m² decreasing with increasing irradiance levels reaching 5% at 1.1 kW/m². We mentioned earlier that the power rating of SW modules was underestimated by 1.7% compared to the FTR which explained only partly the performance difference between the two monocrystalline modules. This suggests a possible overestimation of the ST power ratings and a variation of performance between the two manufacturers, increasing at low irradiance levels. The monocrystalline plots show better performance at low irradiance levels than the HIT, polycrystalline and the amorphous modules. The HIT modules have the most constant PR with the irradiance levels from 200 W/m² to 1.1 kW/m².

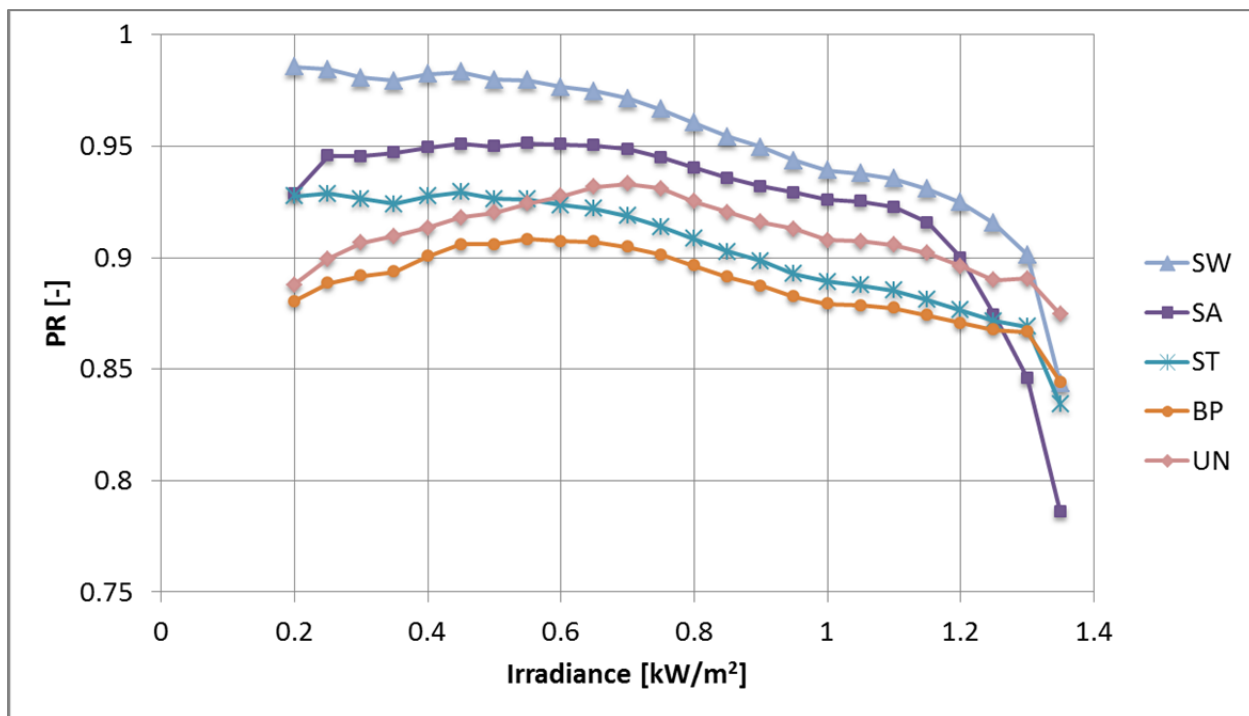


Figure 6: Average PR as a function of levels of irradiance – All PV modules tested at PWW during spring and summer months from July 2010 to March 2012.

3.1.2.2 Impact of the weather conditions

The irradiation (a) and the performance of the PV modules (b-f) tested at PWW as a function of irradiance levels for different weather conditions (all days, sunny, and cloudy) are shown in Figure 7.

The irradiation in spring/summer months is slightly higher than the 21-month average, estimated at $3.8 \pm 1.2 \text{ kWh/m}^2/\text{day}$. Sunny days are selected with irradiation above the average irradiation plus its standard deviation ($> 5.0 \text{ kWh/m}^2/\text{day}$). Cloudy days have irradiation below the average irradiation minus its standard deviation ($< 2.6 \text{ kWh/m}^2/\text{day}$). Cloudy days collect most of the solar energy at low irradiance levels below 500 W/m^2 . Sunny days shift the solar energy at high irradiance levels with a peak at 1 kW/m^2 . All days collect energy at all irradiance levels showing two peaks at 300 W/m^2 and 950 W/m^2 .

For all technologies and all irradiance levels, PR is higher on cloudy days and lower on sunny days compared to the PR for all days. Cloudy days PR shows bumps at irradiance above 900 W/m^2 . This is caused by very short periods of high irradiance levels inducing operation of the PV module at a temperature lower than its normal operating temperature. This phenomenon is also visible on the PR plots on sunny days for irradiance above 1 kW/m^2 . Low irradiance PR degradation on sunny days occurs up to 600 W/m^2 for all PV modules. At 200 W/m^2 , the PR degradation on sunny days is estimated at 4-5% for the monocrystalline, 8% for the polycrystalline, 10% for the HIT and 13% for the UN in comparison to the performance at 600 W/m^2 . On cloudy days, the impact of the low irradiance levels on the PR also varies with the PV technology with variation compared to the performance at 600 W/m^2 estimated at -0.7% for the polycrystalline, 0.3% for the amorphous, 0.9% for the HIT and 2.8-3.2% for the monocrystalline.

The performance at low irradiance levels of the PV modules operating at PWW depends on the PV technology and weather conditions:

- The monocrystalline PR exhibits the lowest degradation for all weather conditions. There is a slight performance difference between the two monocrystalline modules, with higher performance of the SW modules at low irradiance levels in all weather conditions compared to the ST module.
- The HIT and amorphous modules maintain good performance on cloudy days but show higher impact of the low irradiance levels on sunny days compared to the other tested technologies. The HIT exhibits less degradation in all weather conditions compared to the amorphous.
- The polycrystalline is the poorest performing at low irradiance on cloudy days compared to the other technologies tested at the site.

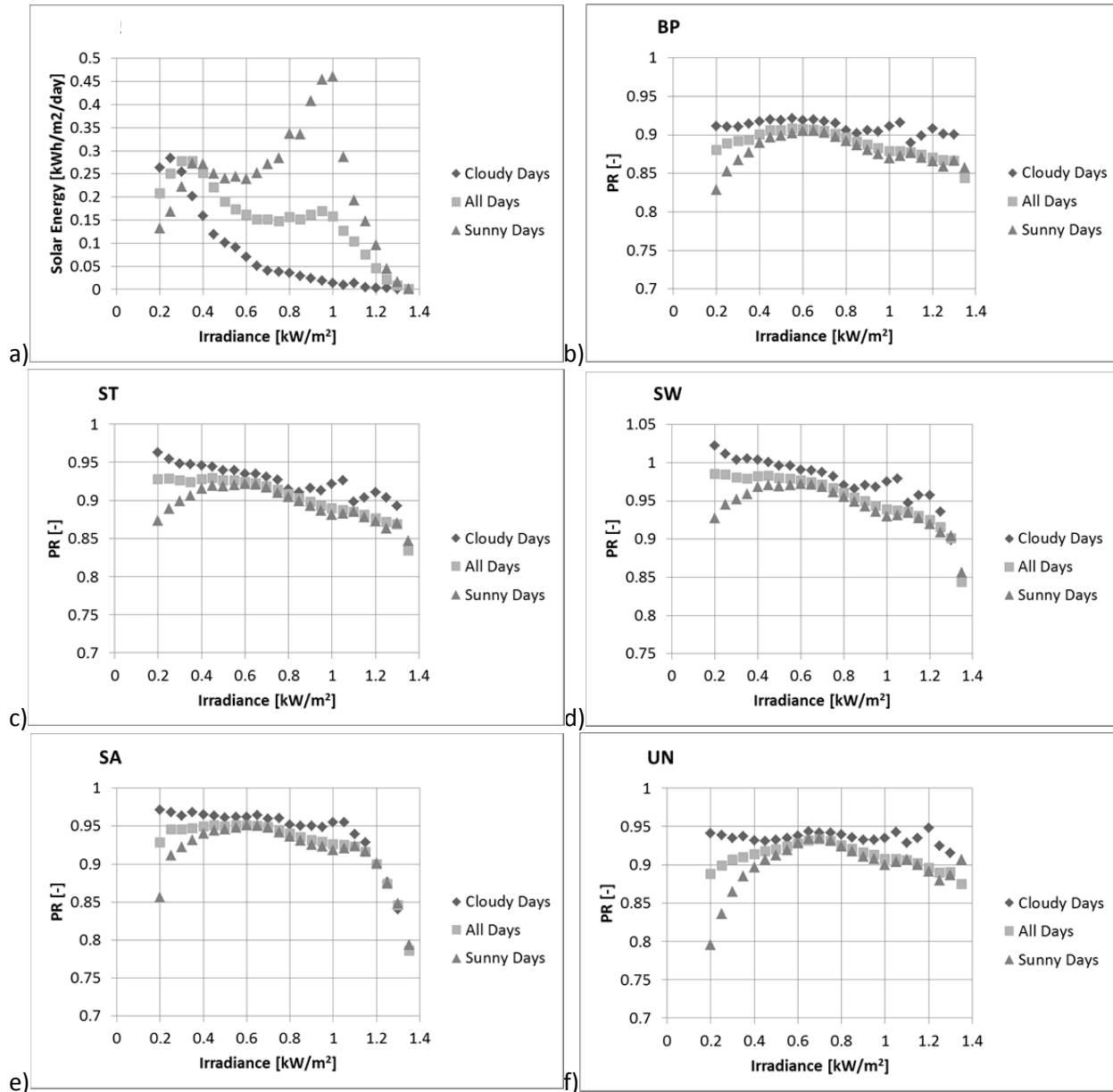


Figure 7: Impact of the weather conditions on the irradiation and PR of the PV modules operating at PWW during spring and summer months of the 21-month period of analysis. a) Irradiation, b) polycrystalline (BP), c) monocrystalline (ST), d) monocrystalline (SW), e) HIT (SA), and f) amorphous (UN)

Table 5: Impact of the weather conditions on the average PR values of the PV modules operating at PWW during the spring/summer months from July 2010 to March 2012.

PV	Cloudy Days	All Days	Sunny Days
SW	100.4%	96.8%	94.9%
SA	96.3%	93.8%	92.7%
ST	94.6%	91.3%	89.8%
UN	93.6%	91.2%	90.2%
BP	91.2%	89.2%	88.1%

The PR values of the PV modules for different weather conditions (all days, sunny and cloudy) are shown in Table 5. These PR values combine the profile of irradiation and PR as a function of the irradiance levels. As expected, the PR is higher on cloudy days and lower on sunny days compared to the PR on all days. The impact of the weather conditions depends on the PV technology: 3.1% for the polycrystalline (BP), 3.4-3.6% for the HIT (SA) and the amorphous modules (UN), and 4.8-5.5% for the monocrystalline, with 4.8% for the ST and 5.5% for the SW. The impact of the weather conditions on the average PR values is an indicator of the performance at low irradiance levels on cloudy days compared to the performance at high irradiance levels on sunny days. The monocrystalline modules are the most sensitive to the weather conditions at PWW due to their high performance at low irradiance levels on cloudy days and low performance at high irradiance levels on sunny days due to their high TC (0.5%/°C). Lower sensitivity of the UN and HIT modules to the weather conditions is related to the higher performance at high irradiance levels on sunny days due to a low TC (0.2-0.3%/°C). The polycrystalline exhibits low impact of the weather conditions due to the degradation of the performance in both low and high irradiance levels.

3.1.2.3 Monthly variation of the performance

We now evaluate the variation of the performance and impact of the weather conditions during the full period of operation. The variation of the monthly PR of the PV modules tested at PWW during the first 21 months of operation is shown in Figure 8. The error bar indicates the variation of the PR due to the weather conditions as described previously by estimating for each month the performance on cloudy and sunny days. During the first year of operation, the PR variation of the crystalline PV modules (ST, SW, BP) differs from that of the amorphous modules (SA, UN) experiencing light induced degradation (LID). It is difficult to determine the duration and amplitude of LID as it is hard to dissociate the degradation of the PV module from the variation of the performance due to varying environmental conditions. The LID seems to occur mainly during the first month of operation, followed by a period of slow performance degradation over about six months for the HIT modules from SA, and about one year of operation for the amorphous modules from UN. During the second year, all PV modules exhibit similar PR variation with performance lower by 3-4% during summer compared to winter months. At this site, the monthly PR variation is within the same range as the impact of the weather conditions previously estimated between 3-5.5%.

The performance of the PV modules during the 21 months of operation indicated in Table 6 is estimated between 90% and 97%. These PR values are slightly higher by 0.2% (UN) to 0.8% (ST) compared to Table 4 due to the inclusion in the analysis of the second winter months with higher PR values. Table 6 also includes the standard deviation of the daily PR. It is calculated at 1.7% for the polycrystalline (BP), 2.0% for the HIT (SA), and 2.4 - 2.6% for the monocrystalline (SW, ST) and for the roof mounted amorphous modules (UN). The standard deviation of the daily PR includes the monthly variation, the variation due to the weather conditions and the LID.

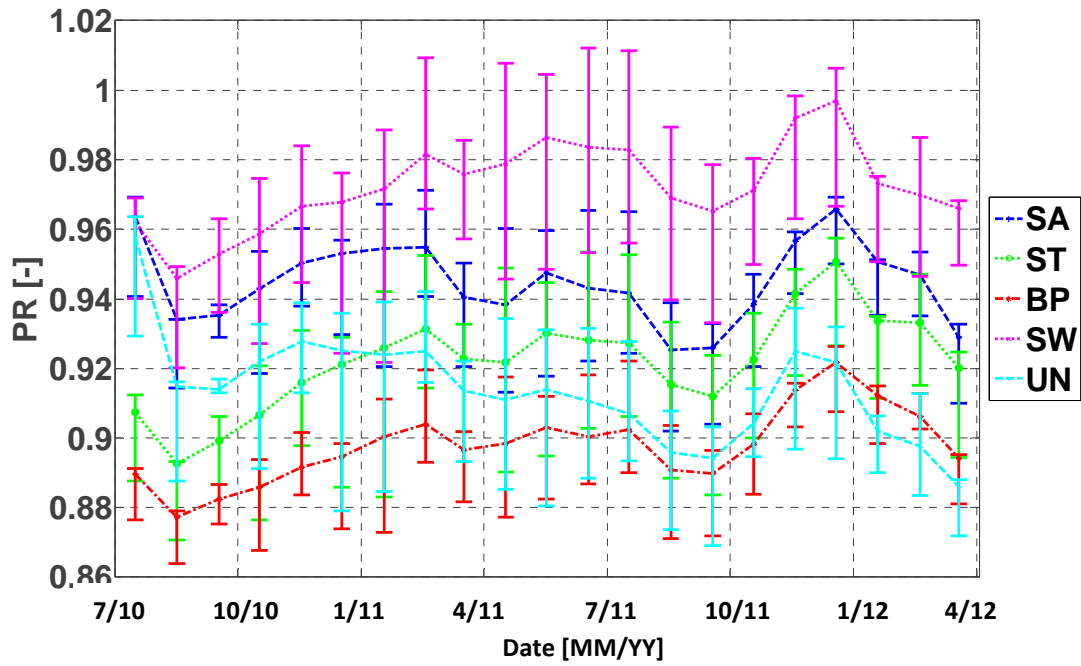


Figure 8: Monthly PR values and impact of the weather conditions for the PV modules tested at PWW during the first 21 months of operation.

Table 6: Average PR and standard deviation of the daily PR for the PV modules tested at PWW during the full period of analysis from July 2010 till March 2012.

PV	Average	STD(period)
SW	97.1%	2.5%
SA	94.4%	2.0%
ST	92.1%	2.4%
UN	91.3%	2.6%
BP	89.7%	1.7%

3.2 Green Holmes Hall Initiative (GHHI), Oahu

The GHHI test site is located at the UH Manoa campus on Oahu on the south side of the mountain slope of the Koolau range (Latitude: 21.3°N, Longitude: 157.8°W, Altitude: 48 m) overlooking Honolulu, two miles from the waterfront (Figure 9).



Figure 9: GHHI, Honolulu, Oahu – PV systems mounted on open rack structure (middle) located on a flat roof on the Koolau Range Mountain slope (background, right image) overseeing Honolulu (background, left image)

GHHI supports side-by-side comparison of two residential-size, grid-tied systems consisting of two different PV module technologies (Table 7). The PV systems consist of the following arrays (Table 8):

- Two parallel strings of 13 polycrystalline PV modules from Kyocera (KYO) connected to a 5 kW SMA string inverter; and
- Six parallel strings of four micro-amorphous PV modules from Mitsubishi Heavy Industries (MHI) connected to a 3 kW SMA string inverter.

PV modules are mounted on open-rack structures, south-facing at an angle of 20°.

Table 7: Description of the PV modules tested at GHHI in Oahu.

PV Module Manufacturers	PV Module Model Number	PV Technology	STC Module Efficiency [%]	STC Peak Power [W]
Kyocera (KYO)	KD205GX-LPU	Polycrystalline	13.8	205
Mitsubishi Heavy Industries (MHI)	MT130	Micro-amorphous	8.3	130

Table 8: Tested PV systems at GHHI in Oahu: Inverter, PV system configuration and PV module mount.

PV	Inverter				PV system configuration			Mount
	Type	Brand	Model	Power [W]	# of inverters	# of PV modules	PV arrangement per inverter	
KY	String	SMA	SB5000US	5k	1	26	2 parallel strings of 13 PV in series	Open rack
MHI	String	SMA	SB3000US	3k	1	24	6 parallel strings of 4 PV in series	Open rack

The PV test bed site was commissioned in December of 2010, and the DAS was commissioned in May of 2011. Since the last report, the DAS at GHHI was improved in order to reduce the noise level. The improved DAS was tested and validated before being fully implemented in April 2012. Recalibration was completed at the test site showing a small deviation of the measurements (< 1%).

The following results correspond to the analysis over two years of operation from October 2011 to September 2013. They include 575 days of analysis. Data loss (~20%) is related to missing or incomplete datasets due to failure or interruption (test period for improvement) of the DAS operation, or to loss of communication. In addition, the analysis is limited to days of proper operation common to all PV systems at the site.

3.2.1 Solar resource

The variation of the daily average irradiation recorded in the plane of the array (20° tilt) from October 2011 to September 2013 at GHHI, with the thermopile pyranometer, is shown in Figure 10. The graph also includes the monthly average values of the irradiation and its standard deviation. The daily irradiation averages $5.8 \text{ kWh/m}^2/\text{day}$. The monthly average irradiation indicates higher solar resources during spring and summer months. The standard deviation varies slightly during the period of recording with higher variation during winter months, averaging at $1.2 \text{ kWh/m}^2/\text{day}$, similar to the previously described test site located in Hawaii.

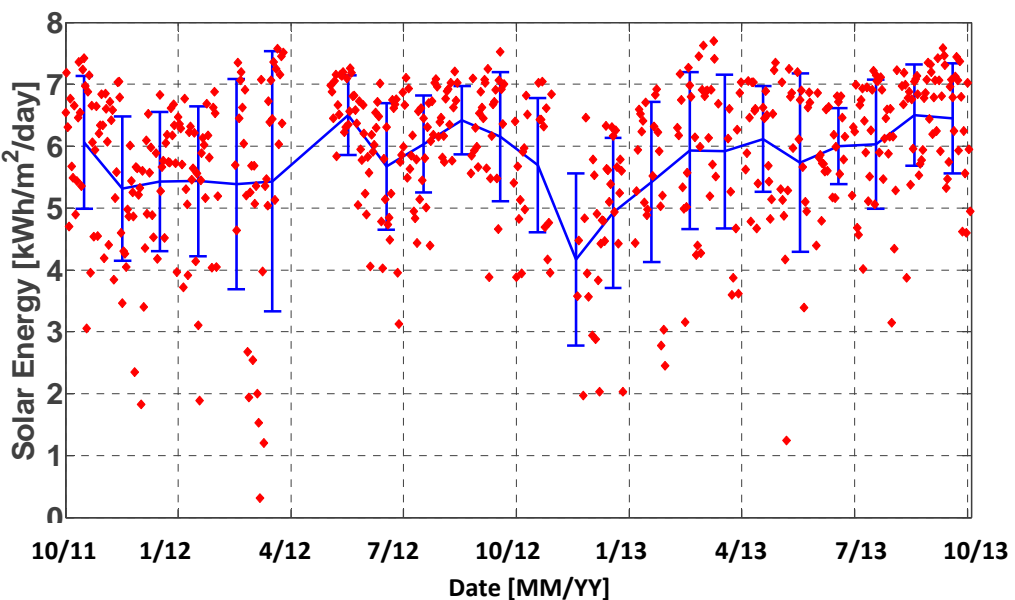


Figure 10: Daily average irradiation with monthly average and standard deviation at GHHI for two years of recording from October 2011 to September 2013. Also shown are monthly averages and standard deviation bars.

The five-minute average solar radiation as a function of hour of the day (y-axis) during the period of analysis (x-axis) is shown in Figure 11. There is no data available before 6:30AM or after 6:30PM due to the consideration in the analysis of the datasets with irradiance levels above 125 W/m^2 in order to maximize the signal to noise ratio of the pyranometer. The dawn and dusk lines vary with the day of the year, which is related to the earth-sun tilt and local shading. Seasonal shading is not as important at this site compared to the test site on Hawai'i Island.

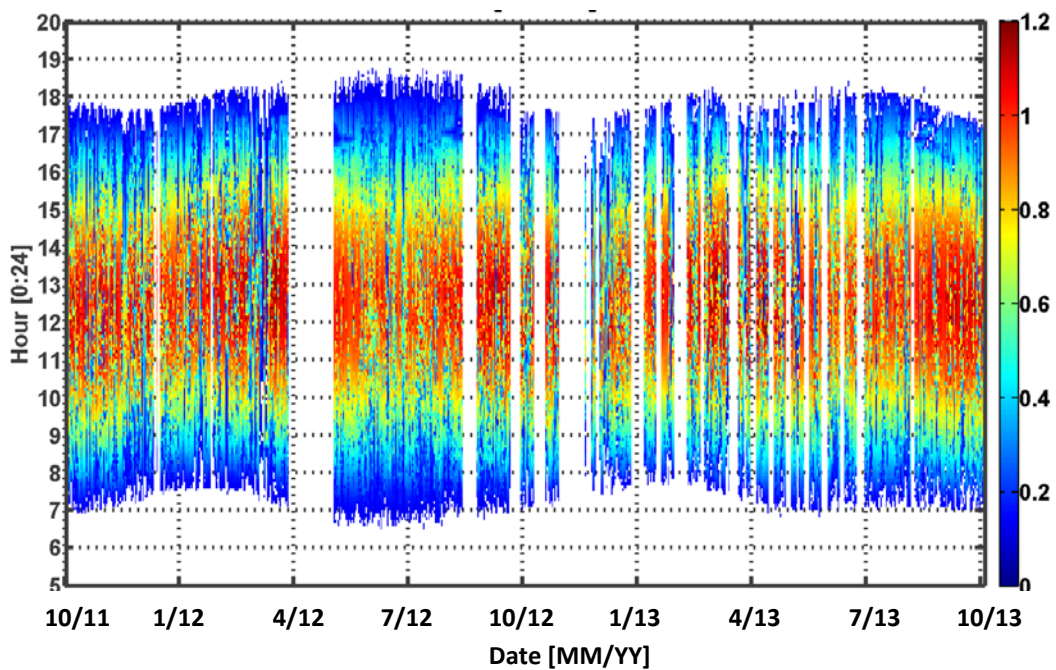


Figure 11 Solar maps at GHHI, Oahu: 5 minute average solar radiation [kW/m^2] varying as a function of hours of the day (y-axis) during the period of analysis from October 2011 to September 2013 (x-axis)

The average and standard deviation of the solar radiation calculated over the two-year period of analysis as a function of the time of the day is plotted in Figure 12. GHHI irradiance levels are high throughout the year, averaging over 800 W/m^2 in the hours around midday. Solar conditions at this test site are consistently sunny during the day and year with variation of the irradiance levels throughout the day due to passing clouds.

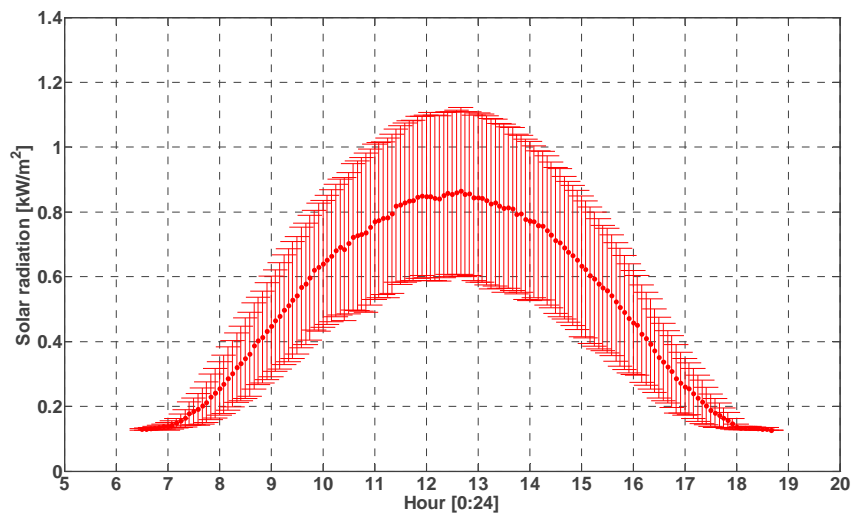


Figure 12: Average and standard deviation of the solar radiation as a function of hour of the day during the 2 years of analysis at GHHI.

3.2.2 Performance of the PV systems

At this site, we observed slight shading of the KYO array in the morning and in the afternoon due to its location in the second and third rows of the PV system (Figure 9). There is more important shading during summer afternoons due to the shade of a building located on the south west of the PV system. In order to compare the performance of the two arrays without shading, we analyzed the performance between 9 AM and 4 PM for the two years of analysis. The impact of the hours of analysis on the irradiation collected per levels of irradiance, showing a difference on the irradiation up to 800 W/m^2 , is shown in Figure 13. Between 9 AM and 4 PM, the average irradiation is estimated at $4.8 \text{ kWh/m}^2/\text{day}$, 14% lower than the full day irradiation. The PR calculated between 9 AM and 4 PM is increased by 0.6% for the micro-amorphous (MHI) and by 1.0% for the polycrystalline array (KYO) compared to the full day PR, due to the operation at low irradiance levels and to the impact of shading for the KYO array.

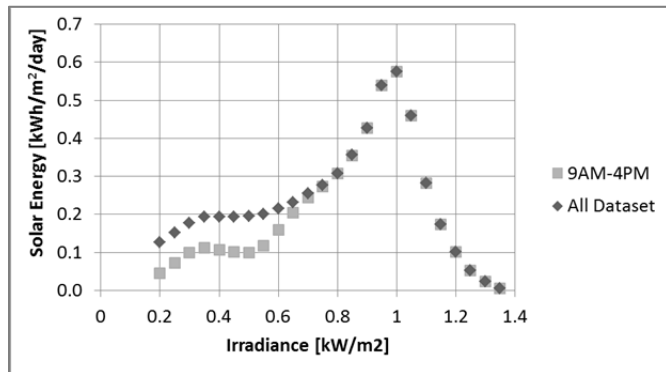


Figure 13: Impact of the hours of analysis on the irradiation collected per level of irradiance at GHHI

3.2.2.1 Average performance

Table 9 shows the average PR of the PV arrays operating at GHHI calculated using data between 9 AM and 4 PM for the two -year period of analysis from October 2011 to September 2013.

Table 9: Average PR of the 2 PV arrays operating at GHHI over 2 years of operation (9AM-4PM) - PR on year 1 (Y1), year 2 (Y2), and over the complete period of analysis (2Y)

PV System	Y1	Y2	2Y
KYO	88.8%	88.4%	88.6%
MHI	85.3%	83.5%	84.5%

The PR is estimated at 88.6% for the KYO array and 84.4% for the MHI array. From year 1 to year 2, the PR decreased by 1.8% for the micro-amorphous (MHI) and by 0.4% for the polycrystalline (KYO). The PR variation from the first to second year can come from a combination of factors, from different operating conditions, aging and soiling, as well as different accuracy or amount of data for each year of operation. The FTR were obtained for the KYO PV modules. The deviation of the power rating from the datasheet specifications is found to average 1.1% for both strings. All KYO PV modules are underrated, with a maximum deviation up to 1.6% of the power rating.

The two -year average PR of the PV arrays operating at GHHI as a function of irradiance levels is plotted in Figure 14. The results are plotted for irradiance levels above 300 W/m² in the following graphs due to the low amount of data below 300 W/m² between 9 AM to 4 PM. Both PV systems have a peak performance between 600 and 800 W/m², estimated at 90% for the KYO and 84-85% for the MHI. The micro-amorphous array shows lower degradation in both low and high irradiance levels compared to the polycrystalline array. This is mainly due to different TC at high irradiance levels. MHI specifies a TC at 0.3%/°C. The TC of the KYO is not specified in the datasheet but should be around 0.5%/°C, as with a crystalline PV module. At low irradiance levels, the different PR degradation between the 2 technologies is due to different spectral response, reflection and recombination. Mismatch loss is another performance parameter of the PV array. It is due to the deviation of the performance of the PV modules connected in series, limiting the string current to the least performing PV module. The FTR of the KYO indicates that the least performing PV module has a current (at maximum PV power) estimated 0.3-0.4% lower compared to the average current between the 13 PV modules in the same string. Above 1.2 kW/m², the PR of both PV arrays drops due to the inverter saturation. In the previous report [2], we estimated the impact of the inverter saturation to be negligible for both arrays with PR degradation of less than 0.2%.

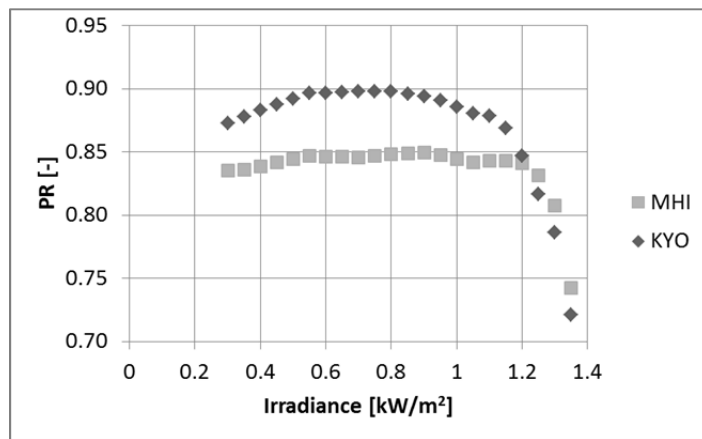


Figure 14: 2-year average PR as a function of irradiance levels – KYO and MHI arrays operating at GHHI between 9AM-4PM from October 2011 and September 2013.

3.2.2.2 Impact of the weather conditions

Figure 15 shows the impact at all irradiance levels of the weather conditions on the irradiation (a) and the PR of the PV arrays (b, c) operating at GHHI from October 2011 to September 2013 (9 AM-4P M). On cloudy days, the irradiation is collected at all levels of irradiance with a peak at 350 W/m². On sunny days, the irradiation is collected at all levels of irradiance with a peak at 1.1 kW/m². For all days, the irradiation at UH Manoa is collected for all irradiance levels but mostly at high levels due to the mostly sunny weather conditions at the site. The predominant irradiance level at GHHI is estimated to be 1 kW/m². For both arrays and at most irradiance levels, the PR is higher on cloudy days and lower on sunny days compared to the PR for all days. The PR on sunny days is higher than all days PR around 500-

600 W/m², which is related to the limited hours of analysis reducing the low performance operation at rising and setting time especially affecting the PR on sunny days. At low irradiance levels, the MHI array maintains high performance on cloudy days but exhibits PR degradation on sunny days. The PR of the KYO array degrades at low irradiance levels in all weather conditions.

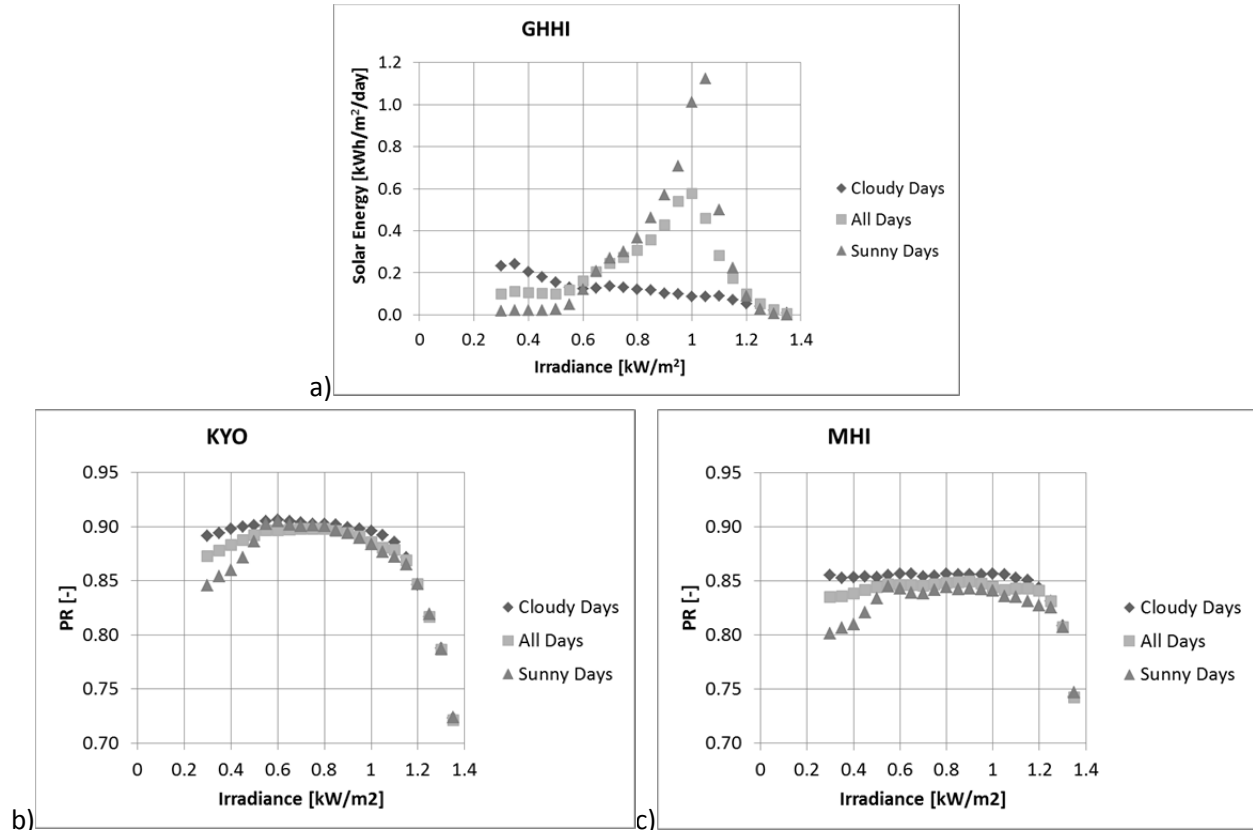


Figure 15: Impact of the weather conditions on the 2-year average PR as a function of irradiance levels for the 2 PV arrays tested at GHHI – 9AM-4PM.

Table 10: Impact of the weather conditions on the PR values of the PV arrays operating at GHHI. 9AM-4PM.

PV	Cloudy Days	All Days	Sunny Days
KYO	89.3%	88.6%	88.5%
MHI	85.5%	84.5%	83.9%

Table 10 shows the PR values monitored for different weather conditions during two years of operation at GHHI (9 AM to 4 PM). These PR values combine the profile of irradiation and PR as a function of the irradiance levels. For both arrays, the PR is higher on cloudy days and lower on sunny days compared to all days PR. Impact of the weather conditions depends on the PV arrays monitored higher for the MHI (1.6%) than for the KYO (0.8%). The micro-amorphous array has high performance at low irradiance levels on cloudy days and shows low PR degradation at high irradiance levels on sunny days due to a low TC (0.3%/°C). The KYO array exhibits PR degradation at low and high irradiance levels in all weather

conditions resulting in low impact of the weather conditions. This result is similar to the observations done at PWW between the amorphous and polycrystalline modules.

3.2.2.3 Monthly variation of the performance

The variation of the monthly PR of the PV arrays tested at GHHI during the two years of analysis using datasets between 9 AM and 4 PM is shown in Figure 16. The error bar indicates the variation of the PR due to the weather conditions by estimating for each month the performance in cloudy and sunny days. The monthly average PR of the KYO array varies between 87.5% and 90%. The PR of the MHI array is mostly impacted by the LID during the first year of analysis and is almost constant around 83-84% during the second year. The impact of the weather conditions is small along the two years of operation with an increased impact during winter months due to higher variation of the irradiation during these periods. The standard deviation of the daily PR is estimated at 1.4% for the KYO array and 1.3% for the MHI reduced to 1.0% during the second year of operation. The standard deviation of the daily PR includes the monthly variation, the impact of the weather conditions and potentially the LID.

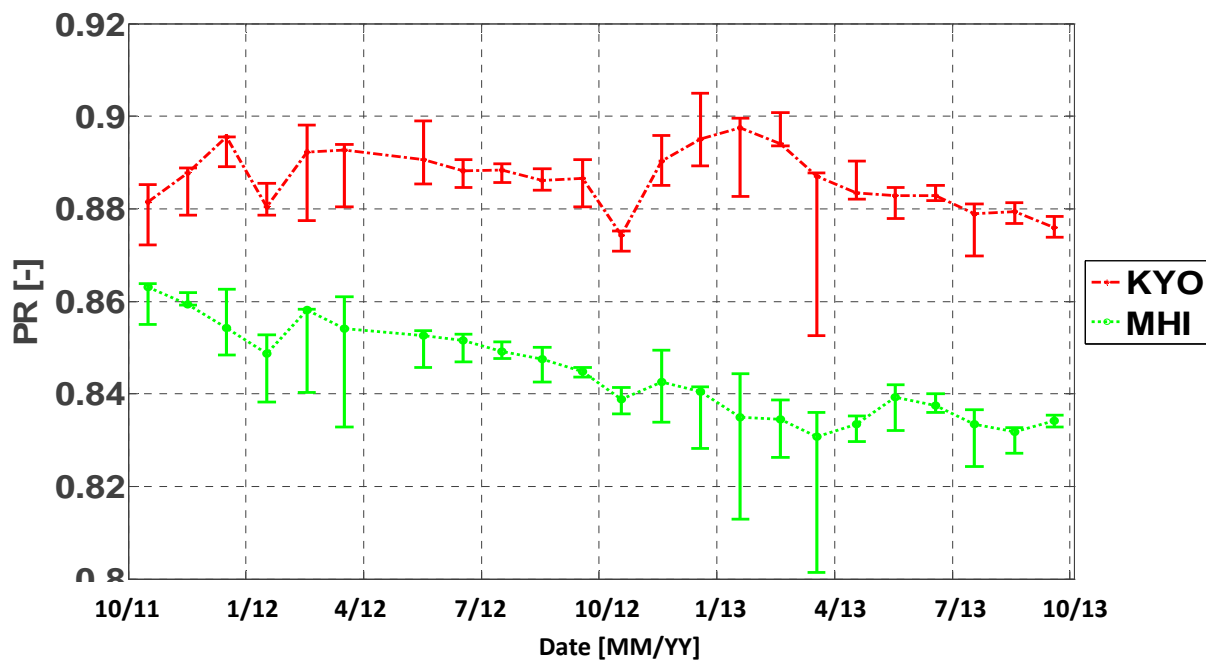


Figure 16: Monthly average of the PR of the PV arrays operating at GHHI during the 2 years of analysis.

4 Conclusions

We analyzed the performance of PV systems at two locations characterized by different solar resource. PWW in Hawaii has sunny mornings and overcast afternoons with an average irradiation of 3.6 kWh/m²/day. The test site GHHI in Oahu is mostly sunny with very consistent weather conditions through the day and year. The irradiation at the Oahu site is estimated at 5.8 kWh/m²/day. At both sites, the standard deviation of the irradiation is estimated at 1.2 kWh/m²/day. The deviation is similar through the period of analysis at PWW and shows higher values during winter months at GHHI.

At PWW, we tested grid-connected PV systems using micro inverters, including PV modules from 5 PV manufacturers and four PV technologies: monocrystalline (ST, SW), polycrystalline (BP), HIT (SA), 3-j amorphous (UN). The average PR of the PV modules is estimated between 90% and 97% as a function of the PV modules. The daily PR varies by 3-5.5% due to the weather conditions (sunny versus cloudy days) and by 3-4% due to the monthly variation of the environmental conditions. The performance of the amorphous modules is also affected by the LID, mostly occurring during the first month of operation, with additional slow degradation for 6 months for the HIT and 1 year for the amorphous.

At GHHI, we tested two grid-connected PV arrays with string inverters and PV modules from two manufacturers and PV technologies: polycrystalline (KYO), micro amorphous (MHI). The PR of the PV arrays was estimated at 84% (MHI) and 89% (KYO). The PR of the KYO array is mostly affected by the monthly variation of the environmental conditions while the MHI PR varies mostly due to the LID. The impact of the weather conditions is small at this site through the two years of operation, with an increased impact during winter months.

At both sites, we found the performance relative to the level of irradiance to be strongly dependent on the PV technology. These observations are summarized below:

At PWW:

- Monocrystalline: STC Efficiency -- 13.4% (SW), 13.7% (ST)
These are good performers at low irradiance levels, but have a high temperature coefficient (TC: 0.5%/°C), exhibiting PR degradation at high irradiance levels. This technology is the most impacted by weather conditions at the site. There are slight performance differences between the two monocrystalline modules, varying with the irradiance levels.
- Polycrystalline: STC Efficiency 13.9% (BP)
This technology is the least sensitive to weather conditions at the site because it exhibits performance degradation in both low and high irradiance levels (TC: 0.5%/°C).
- Amorphous: STC Efficiency 6.1% (UN)
These are good performers at low and high irradiance levels (TC: 0.2%/°C), but show higher loss at low irradiance levels on sunny days compared to the crystalline modules.
- HIT: STC Efficiency 16.7% (SA)
The mixed technology, coupling amorphous and n-type monocrystalline, shows good performance at both high and low irradiance levels. In comparison with the monocrystalline,

the HIT is slightly lower performing at low irradiance levels, especially on sunny days, but is better at high irradiance levels due to a lower TC ($0.34\%/\text{^\circ C}$). The lower TC may be related to the n-type monocrystalline material used by the manufacturer.

At GHHI:

- Polycrystalline: STC Efficiency: 13.8% (KYO)

This technology exhibits performance degradation at low and high irradiance levels. It is the least impacted by weather conditions at the site.

- Micro-amorphous: STC Efficiency: 8.1% (MHI)

This technology shows good performance at low and high irradiance levels due to a low TC ($-0.3\%/\text{^\circ C}$). It is the most impacted by weather conditions at the site due to its good performance in cloudy conditions.

The observations on the amorphous and polycrystalline are similar at the two locations, despite the different solar resource and PV system configurations at the two test sites. The PR versus irradiance plots are very different between the two locations (Figure 6 and Figure 14). Additional test beds will be needed to determine whether the differences are due to the solar resources and/or the PV system configurations. This would require testing PV systems using the same PV modules with different system configurations, replicating the same test bed at more than one location.

Additional improvements of the test protocol are also necessary in order to facilitate the evaluation of the actual power rating of the PV modules. The average PR values presented in this report were calculated compared to the power rating specified in the datasheet of the PV modules. The actual power rating obtained by the available FTR was estimated at about 1-2% above the datasheet specifications, which has a direct impact on the PR values. Using the FTR rating would be more appropriate for performance comparisons between PV systems, but another problem concerns the amorphous technologies that experience LID during the first months of operation and therefore would not benefit from using the FTR in the PR calculations. The solution is to evaluate the actual power of the PV modules using an IV tracer on site. In future experiments, we will characterize the initial power of all PV modules tested in the test beds, and monitor the power of a representative sample of the tested PV modules, allowing the determination of the power variation through the lifetime of the PV module and facilitating the determination of the LID. The IV tracer would also give additional information on the losses in the PV modules as a function of variable environmental conditions [6].

In addition to the improvement of the test protocol, this work has led to new requirements for the DAS for PV test sites that would allow the comparison of the performance of PV systems operating in different locations. A new DAS, presently in validation phase, was designed with low sensitivity to noise, high data collection ability, and high adaptability to various PV system configurations (micro inverters, string inverters, optimizers). This DAS will collect a large number of performance parameters, similar to the present DAS but with additional monitoring on the AC side of the inverters to evaluate the AC PR of the PV systems, as well as estimate the reactive power as a function of PV system configurations. A

calibration unit is also being developed that will permit frequent on-site recalibration of the DAS. An additional product of this project is the development of hardware and software tools that allow automated data collection and archival. Automated data visualization and analysis should also be set up, in order to facilitate the identification of issues with sensors or PV system operation, thus allowing better maintenance of the test sites and reduction of data loss.

5 References

- [1] PV Test Protocols and Data collection, Task 8 Subtask 11.1 Deliverables 1 & 3 for the United States Department of Energy *Hawai'i Distributed Energy Resource Technologies for Energy Security*, DE-FC26-06NT42847, December 2012. Available at:
<http://www.hnei.hawaii.edu/sites/web41.its.hawaii.edu/www.hnei.hawaii.edu/files/page/2012/12/121220%20Task%208%20Deliverable%20and%20Subtask%201.1%20Deliverables%201%20and%203.pdf>
- [2] Solar Resource and PV Systems Performance at Selected Test Sites, Task 8 Subtask 11.1 Deliverables 2 & 4 for the United States Department of Energy *Hawai'i Distributed Energy Resource Technologies for Energy Security*, DE-FC26-06NT42847, December 2012. Available at:
<http://www.hnei.hawaii.edu/sites/web41.its.hawaii.edu/www.hnei.hawaii.edu/files/page/2012/12/121228%20Task%208%20Deliverable%20and%20Subtask%201.1%20Deliverables%202%20and%204.pdf>
- [3] http://files.sma.de/dl/9524/HF_STP_Par-eng-TUS114810.pdf
- [4] <http://www.unidata.ucar.edu/software/netcdf/>
- [5] <http://www.apogeeinstruments.com/content/SP-110manual.pdf>
- [6] S. Busquet, L. Cutshaw, R. Rocheleau, "On the Comparison of the Performance of PV Systems in Hawaii", 28th EU PVSEC 30 Sep-04 Oct 2013 Paris, France.